Fabrication and Microwave Absorption Properties of $Fe_{0.64}Ni_{0.36}$-$NiFe_2O_4$ Nanocomposite

Xu Yan,   Desheng Xue*

Abstract: $Fe_{0.64}Ni_{0.36}$-$NiFe_2O_4$ nanocomposite was performed with partially reducing $NiFe_2O_4$ nanoparticles in Ar/H_2 ambient. The microwave and static magnetic properties were investigated. The results showed that the nanocomposite was characterized with enhanced microwave absorption properties. The optimal reflection loss (RL) of the nanocomposite reached -24.8 dB at 14 GHz for an absorber thickness of 1.5 mm. Meanwhile, a broad bandwidth for RL<-10 dB was obtained in the range of 3.1—15.1 GHz for an absorber thickness from 1.0 to 4.0 mm. The enhancement is attributed to the increase of dielectric and magnetic loss after reducing procedure.
Keywords: $Fe_{0.64}Ni_{0.36}$/$NiFe_2O_4$; Nanoparticles; Microwave

Introduction

With the rapid development of microwave shielding technology in solving the electromagnetic interference pollution problem, huge interests have been focused on ferromagnetic materials based absorbents. In the recent years, Ni/ZnO [1], Co/ZnO [2], Fe/ZnO [3], $FeNi_3/(Ni_{0.5}Zn_{0.5})Fe_2O_4$ [4] and Fe/SiO_2 [5] have been well studied. These nanocomposites are prepared with ferromagnetic nano-cores and dielectric shells, the core acts as a magnet and increases the permeability of the nanocomposites contributing to the magnetic loss, while the shell is not only used as insular which prevents the conjunction of neighbor cores but also a center of electric polarization resulting in the enhanced dielectric loss. The combination of the ferromagnetic and dielectric materials greatly enhances the microwave absorption properties. However, these methods are complex or critical conditions required, therefore are not suitable for mass production.

In this paper, we attempted to prepare the ferromagnetic-dielectric nanocomposite with a quite new method. The dielectric nickel ferrite nanoparticles were fabricated, and then reduced in Ar/H_2 ambient for a short time. The partial of a nickel ferrite nanoparticle was reduced to $Fe_{0.64}Ni_{0.36}$ alloy. The mass ratio of two phases can be controlled by the reducing time. The static magnetic and microwave absorption properties were investigated. The results showed that the nanocomposite was characterized with enhanced microwave absorption properties.

Experimental setup

Nickel ferrite nanoparticles were prepared by sol-gel method [6]. The precursor was annealed at 500℃ for 15 minutes, then the as-prepared powders were reduced in Ar/H_2 ambient for 10 minutes at 400℃ (the flow rate ratio of Ar to H_2 is 50:30), then cooled down to room temperature with Ar atmosphere protection. The as-prepared nickel ferrite nanoparticles was named sample A, and the reduced nanoparticles was named sample B. The X-ray diffraction (XRD) patterns were measured on Philips Panalytical X'pert diffractometer with

$Cu~K\alpha$ radiation. The nanoparticle images were taken by transmission electron microscope (TEM, JIM-2010). The static magnetic properties were investigated by Vibrating Sample Magnetometer (VSM, Lakeshore 7300). The samples for microwave electromagnetic properties measurement were mixed with paraffin (the mass ratio of sample to paraffin is 1:1), and compressed into ring shape with 7.00 mm outer diameter, 3.00 mm inner diameter and 2 mm thickness. The scattering parameters (S11, S21) were measured by a network analyzer (Agilent Technologies E8363B) in the range of 0.1-18 GHz. All of the measurements were performed under the room temperature.

Results and discussion

Figure 1(a) shows the TEM image of sample A. The nanoparticles' average diameter is about 20 nm. The TEM micrograph of sample B is shown in Fig. 1(b), an obvious increase of the average diameter is observed. Figure 1(c) shows the XRD patterns of the two samples. Single spinel $NiFe_2O_4$ phase was observed in sample A. After partially reducing process, fcc $Fe_{0.64}Ni_{0.36}$ phase and spinel $NiFe_2O_4$ phase coexisted in sample B. According to Scherrer's formula and the full width at half-maximum (FWHM) of (311) peak, the average grain size of $NiFe_2O_4$ was estimated to be 21 and 53 nm for sample A and sample B, respectively. The increase of grain size between the two samples may be at-

tributed to the annealing in partially reducing process. Figure 1(d) illustrates the magnified image of nanoparticle in sample B. The inter-planar space of the particle in the Section I is 0.486 nm, which corresponds to the (111) plane of $NiFe_2O_4$ with spinel structure. However, with the inter-planar space of Section II and III can not be distinguished. The high-resolution image containing Section II and III is shown in Fig. 1(e). The lattice with inter-planar spaces of 1.78 and 2.02 nm in Section II can be identified as the (111) and (200) planes of $Fe_{0.64}Ni_{0.36}$ respectively, and the lattice with inter-planar spaces of 2.51 nm in Section III can be identified as the (311) plane of $NiFe_2O_4$. The results well agree with the XRD data. Thus, it can be speculated that parts of $NiFe_2O_4$ nanoparticles in sample A merged into large particle in the heating process under partly reduction, which led to the increase of average diameter and grain size in sample B. When the large particles were in Ar/H_2 atmosphere, the surfaces of these particles were reduced to $Fe_{0.64}Ni_{0.36}$ alloy. After the partial reducing process, the sample was cooled down to room temperature. Then it was exposed in the air ambient. The surfaces of the $Fe_{0.64}Ni_{0.36}$ alloy were passivated into $NiFe_2O_4$, and the thickness of the passivated layer is about 4 nm. The reduced $Fe_{0.64}Ni_{0.36}$ phase was embodied in the $NiFe_2O_4$ nanoparticles. Figure 1(f) illustrates the selected area electron diffraction (SAED) patterns of sample A and B, the results well agree with the data of XRD.
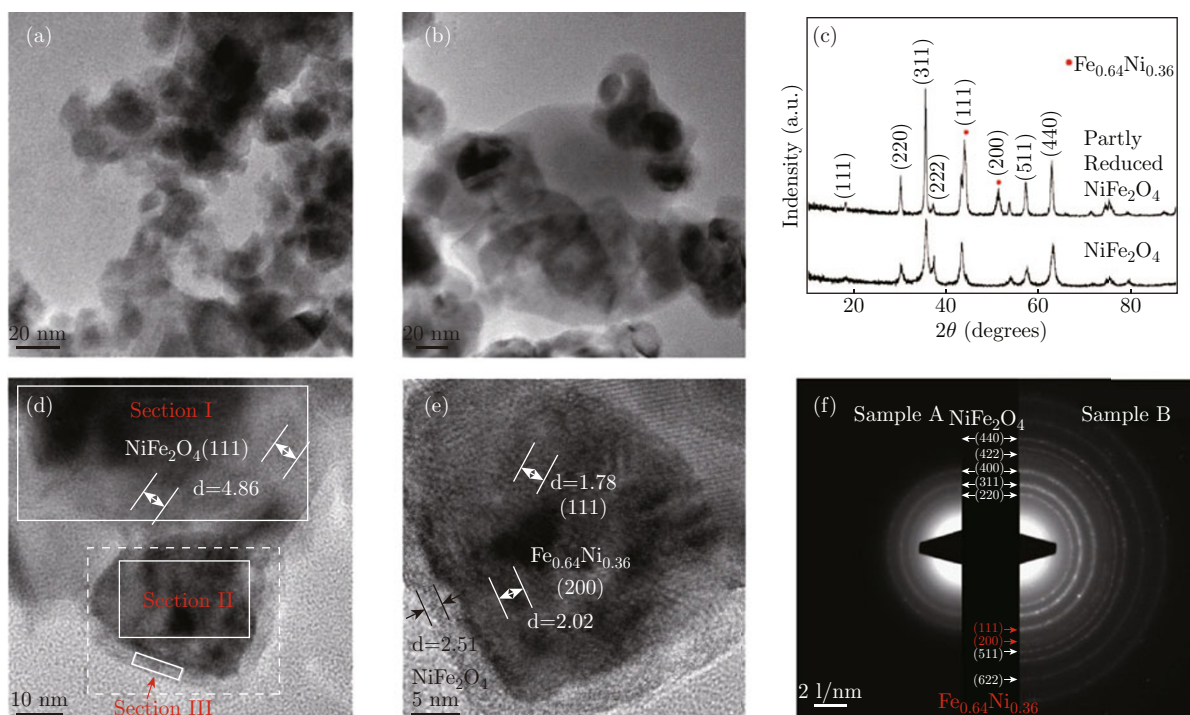

Fig. 1   TEM images of sample A (a) and B (b), XRD patterns of sample A and B (c), HRTEM images of sample B (d and e) and SAED patterns of sample A and B (f).

Figure 2 shows the hysteresis loops of sample A and B. After partially reducing procedure, the saturation magnetization (M_S) of the sample B increased from 32 to 78 emu/g, the coercivity was enhanced from 61 to 195 Oe. The M_S of $Fe_{0.64}Ni_{0.36}$ nanoparticles was reported to be 126.8 emu/g [7]. According to the M_S of sample A, B and $Fe_{0.64}Ni_{0.36}$ nanoparticles, the weight ratio of $Fe_{0.64}Ni_{0.36}$ in the sample B was calculated to be 48.5%.
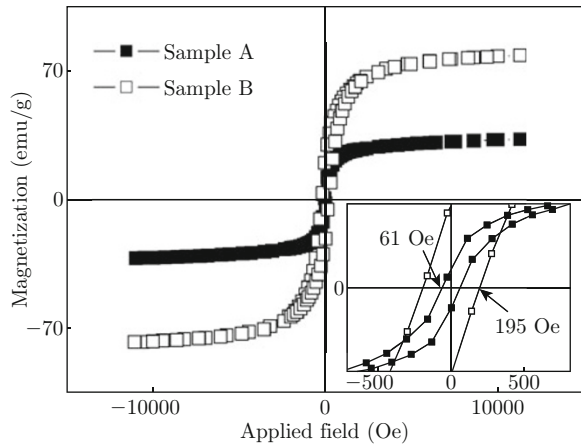

Fig. 2   The hysteresis loops of sample A and B, the inert indicates the enlarged part of coercivity.

Figure 3(a) exhibits the real and imaginary parts (ε', ε'') of complex permittivity spectra of the two sam-ples. The solid square corresponds to the sample A, and the red circle presents the sample B. The ε' and ε'' of sample A both show a decrease when the frequency is lower than 1 GHz and then keeps almost constant in the following measured range. It can be noticed that both ε' and ε'' of the sample B are higher than those of the sample A throughout the measured range, that's to say, the energy loss in the sample B is enhanced in which ε'' represents dielectric loss. In this study, the partially reduced $Fe_{0.64}Ni_{0.36}$ in the sample B increases the conductivity of the sample and contributes to the enhancement of the real part of complex permittivity. On the other hand, the free electrons can accumulate at the interface of the two phases, generating interfa-cial electric dipolar polarization which contributes to the increasing of the imaginary part of the sample B.

Figure 3(b) exhibits the real and imaginary parts (μ', μ'') of complex permeability spectra of the sample A and B. The μ' of the sample A decreases from 1.8 to 0.9 with as the frequency increases from 0.1 to 18 GHz, while the μ' of the sample B decreases from 2.4 to 0.8. The μ'' spectrum of sample A shows a single broad peak at about 3 GHz which can be ascribed to the nat-ural resonance of $NiFe_2O_4$ [8]. In the μ'' spectrum of the sample B, the strongest peak appears at about 2.4 GHz, the second peak is around 12 GHz and the third peak stands at 17 GHz. The peak position of the first peak is close to that of the sample A, and the peak
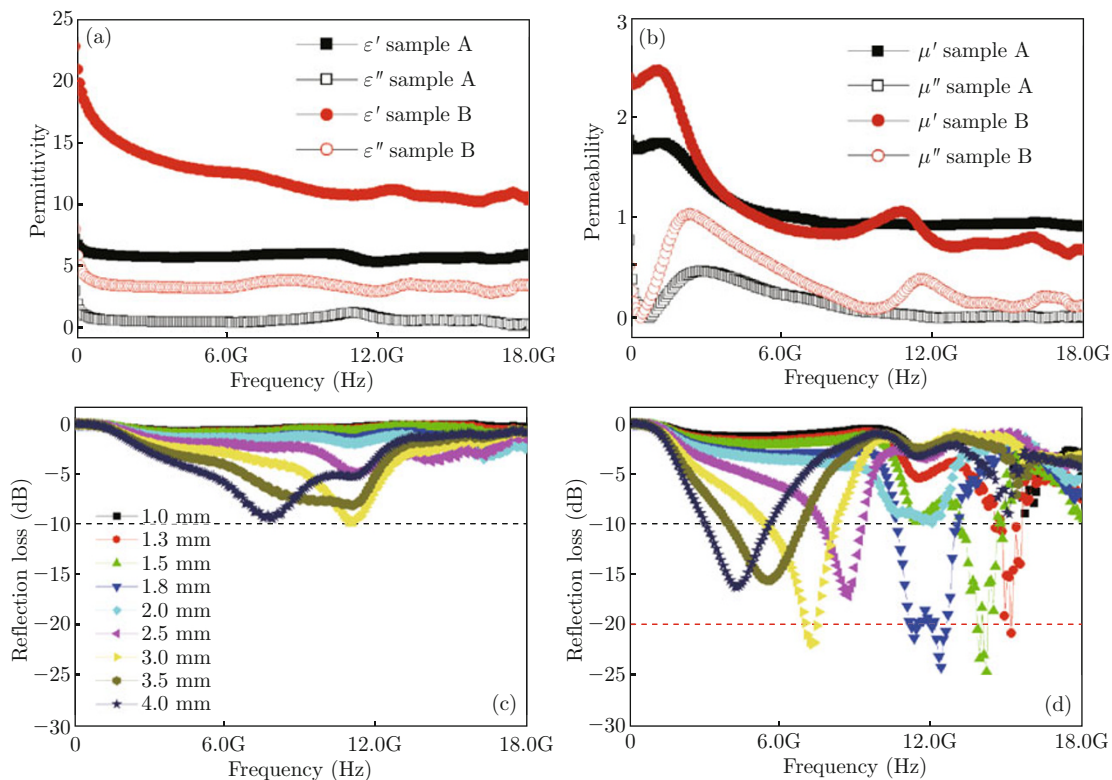

Fig. 3   Frequency dependence of the complex permittivity (a) and permeability (b), the relationship of reflection loss and frequency of the sample A (c) and B (d) for varied thickness.

intensity is about two times more than that of as-prepared nanoparticles. The mass ratio of nickel ferrite in sample B is smaller than that of sample A, the contribution of natural resonance of $NiFe_2O_4$ to μ'' in the sample B also is smaller than that of the sample A. As a result, the strongest peak could be caused by natural resonance of both nickel ferrite and invar alloy. The second and third peak may result from exchange mode of invar alloy [9]. The magnetic loss (μ'/μ'') of two samples have been calculated, the values of partly reduced sample were enhanced in comparison with those of $NiFe_2O_4$ nanoparticles throughout the measured range.

Figure 3(c) shows the calculated reflection loss (RL) of the sample A. The optimal RL is higher than 10 dB. The thickness dependent RL spectra of the sample B are shown in Fig. 3(d). In comparison with the sample A, the optimal RL of the sample B reached -24.8 dB at 14 GHz for a thickness of 1.5 mm. A broad bandwidth for RL<-10 dB was obtained in the range of 3.1–15.1 GHz as the thickness varied from 1.0 to 4.0 mm, covering the whole X-band (9–12.4 GHz). The enhanced microwave absorption properties can be attributed to the increasing of dielectric loss and magnetic loss after partially reducing procedure.

Conclusions

In conclusion, $Fe_{0.64}Ni_{0.36}$-$NiFe_2O_4$ nanocomposite was successfully fabricated by sol-gel and simple thermal reduction process. The results show that the optimal RL of nanocomposite reach -24.8 dB at 14 GHz for a thickness of 1.5 mm and a broad bandwidth for RL<-10 dB was achieved in the range of 3.1–15.1 GHz for a thickness from 1.0–4.0 mm. The nanocomposite is characterized with outstanding microwave absorption properties and convenient preparation method; it owns the great potential of application in the highly efficient microwave absorber.

References

[1] X. G. Liu, J. J.Jiang, D. Y. Geng, B. Q. Li, W. Liu and Z. D. Zhang, Appl. Phys. Lett. 94, 053119 (2009). http://dx.doi.org/10.1063/1.3079393

[2] T. Wei, C. Q. Jin, W. Zhong and J. M. Liu, Appl. Phys. Lett. 91, 222907 (2007). http://dx.doi.org/10.1063/1.2819089

[3] X. G. Liu, D. Y. Geng, H. Meng, P. J. Shang and Z. D. Zhang, Appl. Phys. Lett. 92, 173117 (2008). http://dx.doi.org/10.1063/1.2919098

[4] X. G. Lu, G. Y. Liang, Y. M. Zhang and W. Zhang, Nanotechnology 18, 015701 (2007). http://dx.doi.org/10.1088/0957-4484/18/1/015701

[5] L. G. Yan, J. B. Wang, X. H. Han, Y. Ren, Q. F. Liu and F. S. Li, Nanotechnology 21, 095708 (2010). http://dx.doi.org/10.1088/0957-4484/21/9/095708

[6] A. T. Raghavender, N. Biliškov and Ž. Skoko, Mater. Lett. 65, 677 (2011). http://dx.doi.org/10.1016/j.matlet.2010.11.071

[7] L. H. Bar, J. S. Kim and J. C. Kim, Res. Chem. Intermed. 36, 795 (2010). http://dx.doi.org/10.1007/s11164-010-0183-9

[8] H. T. Zhao, X. D. Sun, C. H. Mao and J. Du, Physica B: Condensed Matter 104, 69 (2009). http://dx.doi.org/10.1016/j.physb.2008.10.006

[9] F. Ma, Y. Qin and Y. Z. Li, Appl. Phys. Lett. 96, 202507 (2010). http://dx.doi.org/10.1063/1.3432441